Zhao, H., et al., 2020, Paleomagnetic insights into the Cambrian biogeographic conundrum: Did the North China craton link Laurentia and East Gondwana?: Geology, v. 49, https://doi.org/10.1130/G47932.1

Online Supplementary Material for:

Paleomagnetic insights into the Cambrian biogeographic conundrum: Did the North China Craton link Laurentia and East Gondwana?

Hanqing Zhao, Shihong Zhang, Maoyan Zhu, Jikai Ding, Haiyan Li, Tianshui Yang, and Huaichun Wu

This file contains:

1. Detailed paleomagnetic statistical parameters
2. Figure DR1
3. Figure DR2
4. Figure DR3
5. Figure DR4
6. Table DR1
7. Table DR2
8. Table DR3
9. Supplementary references

1. Detailed paleomagnetic statistical parameters

For reversals test

The high temperature component (HTC) of the section A in Xuzhou region yields both geomagnetic polarities (Fig. 2C). The sample-mean direction for the 45 samples after bedding tilt correction is *Ds*/*Is* = 150.8°/40.7° (k = 23.1, α_{95} = 4.5°). The antipodal polarities of the HTC passed a positive reversal test at the 95% probability level: γ_o (observed angular difference) = 7.7° <γ_c (critical angle) = 12.4° (class C; McFadden and McElhinny, 1990; Table DR1). The site-mean direction for the 6 sites after bedding tilt correction is *Ds*/*Is* = 150.8°/40.6° (k = 126.0, α_{95} = 6.0°). The antipodal polarities of the HTC also passed a positive reversal test at the 95% probability level: γ_o = 8.2° <γ_c = 9.4° (class B; McFadden and McElhinny, 1990; Table DR1). The mean pole 26.0 °S/147.2 °E (A_{95} = 6.8°) for the Hsuchuang Formation (Fm) in the Xuzhou region was obtained by averaging the virtual geomagnetic poles (VGPs) calculated for each site (Table DR1).

In section B in the Tai'an region, only the polarity-1 directions were identified (Fig. 2C). The sample-mean direction for the 39 samples after bedding tilt correction is *Ds*/*Is* = 171.2°/39.8° (k = 21.9, α_{95} = 5.0°). The site-mean direction for the 6 sites after bedding tilt correction is *Ds*/*Is* = 171.0°/40.0° (k = 62.5, α_{95} = 8.5°). The mean pole 30.4 °S/127.9 °E (A_{95} = 7.3°) for the Hsuchuang Fm in the Tai'an region was obtained by averaging the VGPs calculated for each site (Table DR1).

The 21 site-level VGPs in the five regions of the two polarity groups passed a reversal test at the 95% probability level: γ_o = 2.6° <γ_c = 13.9° (class C; McFadden and McElhinny, 1990; Table DR1).

For regional tilt test

A regional tilt test for the 21 site-level VGPs is positive at 95% and 99% confidence (McElhinny, 1964), Ks/Kg = 18.9685 > F(2*(n2-1),2*(n1-1)) at 5% (1%) point= 1.69 (2.11) (Table DR1). Another regional tilt test is also positive at the 95% and 99% confidence (McFadden, 1990), critical Xi at 95% = 5.34, at 99% = 7.48; Xi1 IS = 13.1, Xi1 TC = 1.04; Xi2 IS = 13.4, Xi2 TC = 3.30 (Table DR1).

We calculate a mean pole for the Hsuchuang Fm at 31.8 °S, 140.4 °E (A_{95} = 5.3°) by averaging 21 VGPs obtained from the five regions (pole "XZ" in Table DR1).

2. Figure DR1

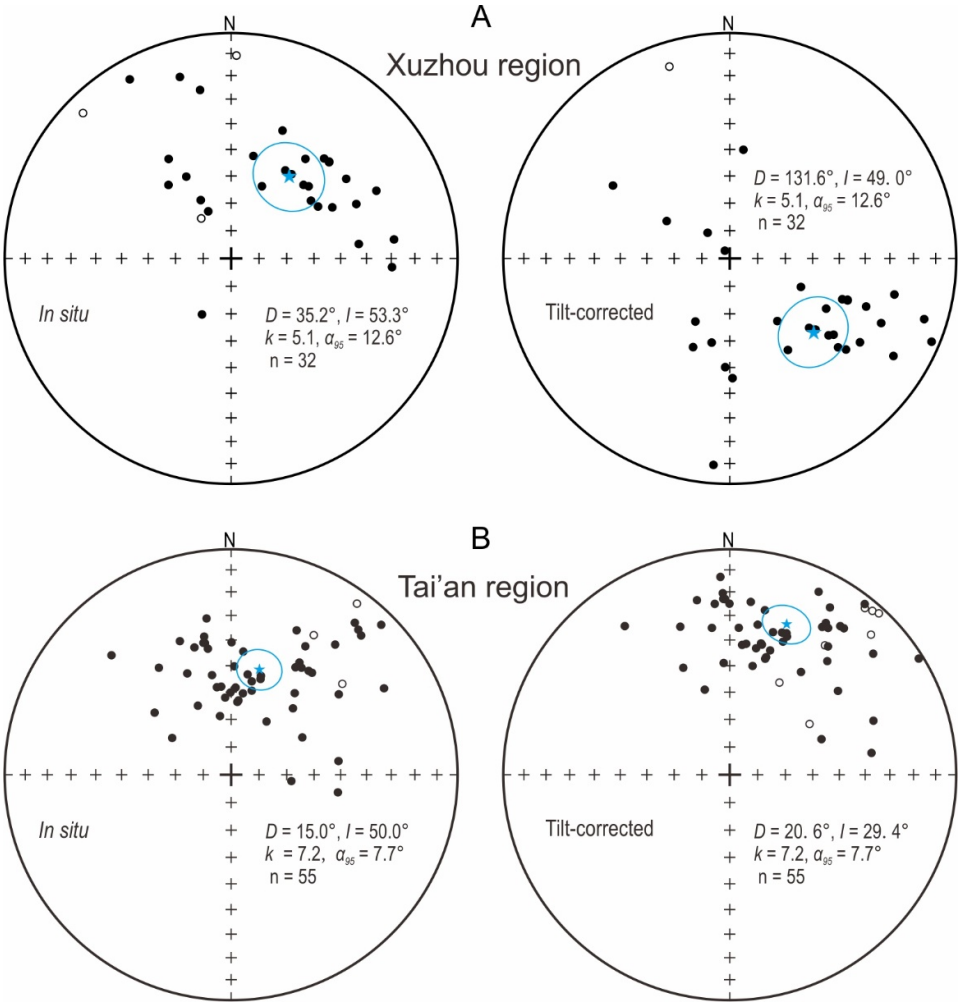

Figure DR1. Equal area projections showing paleomagnetic directions of the low temperature component isolated from the Hsuchuang Formation in (A) the Xuzhou region and (B) the Tai'an region. The stars with 95% confidence circle indicate Fisher statistic directions. *D*—declination; *I*—inclination; α_{95}—radius of 95% confidence cone of the mean direction; n—sample number; *k*—precise parameter. Closed/open symbols represent the downward/upward paleomagnetic inclinations.

3. Figure DR2

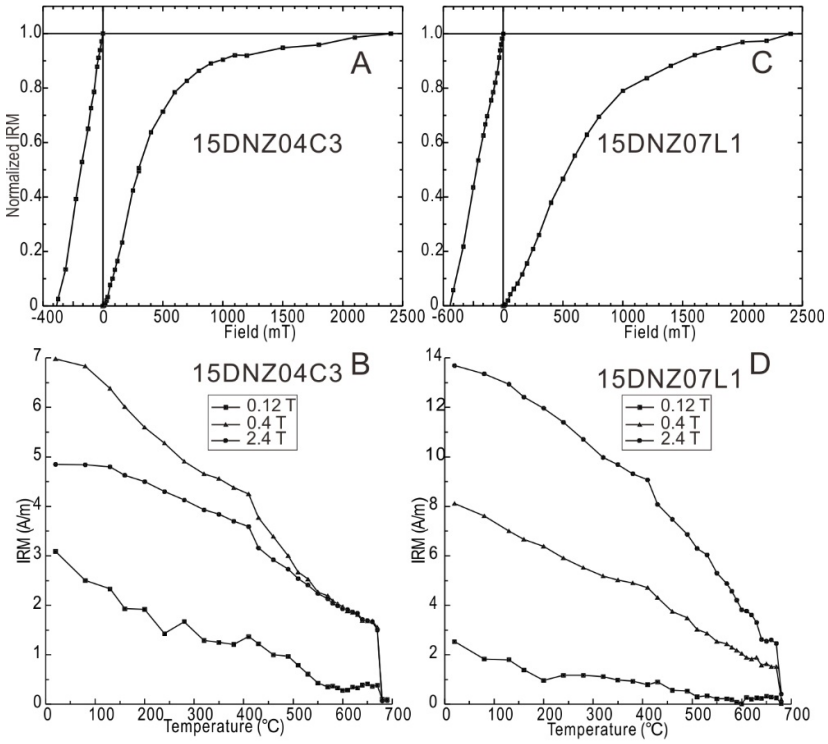

Figure DR2. Rock magnetic results of representative specimens from the Hsuchuang Formation in the Xuzhou region. (A) and (C) Isothermal remanent magnetization (IRM) and back-field demagnetization of saturation IRM (SIRM) acquisition curves. (B) and (D) Lowrie test (Lowrie, 1990; thermal demagnetization of the three-axis IRMs) results.

4. Figure DR3

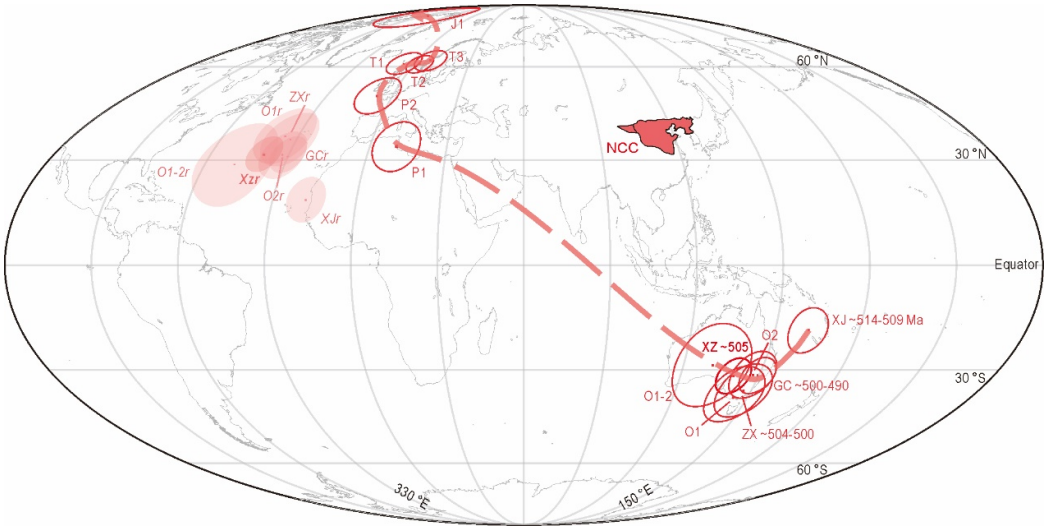

Figure DR3. Cambrian to Early Jurassic (north pole) apparent polar wander path for the North China Craton. The reversed pole positions of the Cambrian and Ordovician poles are shown with pale-pink A_{95} (e.g., pole "XZr"). Cambrian and Ordovician poles are listed in Table DR2. P1 data are from Miao (2015). P2, T1, T2, T3 and J1 data are after Huang et al. (2008). Cambrian pole abbreviations: XJ—pole of the Xinjin and Wudaotang formations; XZ—pole of the Hsuchuang Formation; ZX—pole of the Changhsia Formation; GC—pole of the Kushan and Changshan formations. Geologic time abbreviations: O1–Early Ordovician; O2–Middle Ordovician; P1—Early Permian; P2—Late Permian; T1—Early Triassic; T2—Middle Triassic; T3—Late Triassic; J1—Early Jurassic.

5. Figure DR4

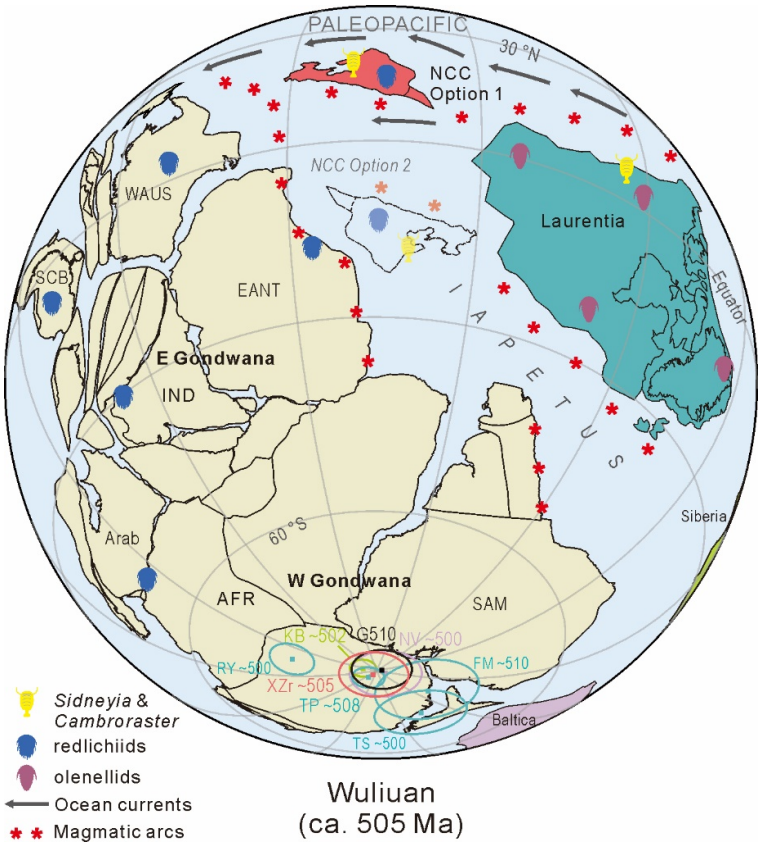

Figure DR4. Southward view of the ca. 505 Ma paleogeographic reconstruction. Global reconstruction is mainly based on the paleomagnetic data (Table DR2). Absolute longitudes for each tectonic entity are arbitrary. Gondwana's pole is in black, while other continents and their poles are matched in color. The pole "XZr" represents the reversed pole of pole "XZ". Ages following pole abbreviations are in Ma. Configuration of Gondwana and peri-Gondwana terranes is modified from Xian et al. (2019). F For Euler rotation parameters seeing in the Data Repository (Table DR3). Distribution of the magmatic arcs are synthesized from Li and Powell (2001); Cawood (2005); Dalziel (2014); Han et al. (2016) and Torsvik and Cocks (2017). Inferred ocean currents are modified from Brock et al. (2000). Distributions of Burgess Shale-type fossils (arthropods *Sidneyia* and *Cambroraster*) are according to Sun et al. (2020a, 2020b). Distributions of redlichiids and olenellids are modified after Sundberg et al. (2020). Term "olenellids" includes families *Olenellidae* and *Biceratopsidae*. Term "redlichiids" includes *Redlichiinae* only. AFR—Africa; Arab—Arabia; EANT—East Antarctica; IND—India; SAM—South America; SCB—South China Block; WAUS—west Australia.

6. Table DR1

TABLE DR1. SITE-MEAN VALUES AND STATISTICAL RESULTS FOR THE HSUCHUANG FORMATION IN THE XUZHOU, TAI'AN, ZHONGYANG, HANCHENG AND JINGXING REGIONS, NORTH CHINA CRATON

					In situ		Tilt-corrected				Tilt-corrected			
Site ID	n	n_0	dip direction	dip	*D*	*I*	*D*	*I*	*k*	α_{95}	Plong	Plat	*dp*	*dm*
			(°)	(°)	(°)	(°)	(°)	(°)		(°)	(°E)	(°N)	(°)	(°)
Xuzhou region (34.463 °N, 117.401 °E)														
Red siltstone (Section A)														
15DNZ02	7	10	171	62	30.7	71.7	155.5	41.2	22.0	13.2	142.7	-27.4	9.8	16.1
15DNZ04	8	14	171	62	14.2	77.2	164.5	39.6	20.0	12.7	134.2	-31.2	9.1	15.2
15DNZ05	7	12	171	62	49.8	66.4	145.3	37.8	17.9	14.7	153.3	-25.3	10.2	17.3
15DNZ07	8	10	171	62	28.4	66.9	151.3	45.0	23.5	11.7	145.3	-23.2	9.4	14.8
15DNZ08	8	11	171	62	234.3	-62.2	319.6	-36.9	33.3	9.7	338.6	22.9	6.6	11.4
15DNZ09	7	10	171	62	217.6	-67.7	329.3	-41.7	44.8	9.1	328.3	24.6	6.8	11.1
Mean of 6 sites*					38.4	69.2	150.8	40.6	126.0	6.0	147.2	-26.0	A_{95} = 6.8	
Mean of 45 samples†					38.3	69.2	150.8	40.7	23.1	4.5	147.3	-25.9	3.3	5.5
Tai'an region (35.736 °N, 117.787 °E)														
Red siltstone (Section B)														
16XT01	6	8	36	20	179.6	24.6	171.3	39.9	31.4	12.2	127.2	-31.0	8.8	14.7
16XT02	6	9	36	20	180.7	12.4	176.1	28.4	27.1	13.1	122.6	-39.0	7.9	14.4
16XT05	6	9	36	23	180.6	13.0	174.8	31.2	23.9	14.0	124.0	-37.2	8.8	15.7
16XT06	7	7	36	23	178.0	32.9	163.5	49.3	32.8	10.7	133.2	-22.3	9.4	14.2
16XT07	5	6	36	23	178.0	35.1	162.2	51.4	22.4	16.5	133.8	-20.2	15.2	22.4
16XT13	9	16	34	22	181.8	21.2	173.8	38.9	21.9	11.3	124.6	-32.0	8.0	13.5

(continued)														
Mean of 6 sites					179.9	23.2	171.0	40.0	62.5	8.5	127.9	-30.4	A_{95} = 7.3	
Mean of 39 samples					180.0	23.0	171.2	39.8	21.9	5.0	127.3	-31.1	3.6	6.0
Zhongyang region, Shanxi (Huang et al., 1999) (37.3 °N, 111.2 °E)														
Sandstone and limestone														
X08	5	-	287	25	154.4	23.1	166.5	38.2	47.5	11.2	125.7	-29.9	7.9	13.3
X10	4	-	287	25	160.5	-7.6	160.5	7.4	21.8	20.1	139.4	-45.1	10.2	20.2
X11	4	-	287	25	350.3	3.9	351.0	-7.4	52.7	12.8	304.7	48.1	6.5	12.9
Hancheng region, Shaanxi (Huang et al., 1999) (35.6 °N, 110.5 °E)														
Sandstone, shale, limestone and dolomitic limestone														
E28	6	-	120	57	173.8	53.9	148.7	8.6	36.3	11.3	153.4	-40.5	5.7	11.4
E30	7	-	120	57	176.4	62.8	143.4	15.8	91.1	6.4	156.2	-34.4	3.4	6.5
E31	5	-	120	57	178.6	60.6	145.8	15.0	85.9	8.3	154.1	-36.1	4.4	8.5
E32	5	-	120	57	189.4	66.6	143.8	22.4	19.6	17.7	153.3	-31.6	9.9	18.8
E33	6	-	120	57	181.8	68.0	140.7	20.9	23.6	14.1	156.8	-30.6	7.8	14.8
Jingxing region, Hebei (Zhao et al., 1992) (38.0°N, 114.1 °E)														
Limestone														
NCB.030	5	-	273	30	322.2	-27.6	341.2	-43.7	36.1	12.9	312.1	23.3	10.0	16.1
XZ (mean of 21 sites)[§]											**140.4**	**-31.8**	**A_{95} = 5.3**	

Note: n–number of samples used to calculate mean; n_0–total samples demagnetized; *D*/*I*–declination/inclination; *k*–precision parameter of Fisher (1953); α_{95}–radius of 95% confidence cone of the mean direction; Plat, Plong–latitude, longitude of the virtual geomagnetic pole (VGP); *dm*, *dp*–semiminor and semimajor axes of 95% polar error ellipse. A_{95}–radius of 95% confidence cone of the paleomagnetic pole.

[*]Pass a reversal test (McFadden and McElhinny, 1990), class B (critical angle γ_c = 9.4°; observed angular difference γ_o = 8.2°).

[†]Pass a reversal test (McFadden and McElhinny, 1990), class C, with a critical angle 12.4°, and observed angular difference is 7.7°.

[§](1) Mean pole (pole "XZ") by averaging the 21 site-level VGPs from the Hsuchuang Formation reported by Zhao et et al., 1992; Huang et al., 1999 and this study; (2) All 21 sites jointly passed a reversal test (McFadden and McElhinny, 1990), class C (critical angle γ_c = 2.6°; observed angular difference γ_o = 13.9°); (3) A regional tilt test is positive at 95% and 99% confidence

(McElhinny, 1964), Ks/Kg = 18.9685 > F(2*(n2-1), 2*(n1-1)) at 5% (1%) point = 1.69 (2.11); (4) A regional tilt is also positive at the 95% and 99% confidence (McFadden,1990), critical Xi at 95% = 5.34, at 99% = 7.48; Xi1 IS = 13.1, Xi1 TC = 1.04; Xi2 IS = 13.4, Xi2 TC = 3.30.

7. Table DR2

TABLE DR2. SELECTED CAMBRIAN TO MIDDLE ORDOVICIAN PALEOMAGNETIC POLES FROM NORTH CHINA CRATON AND CA. 510−500 Ma PALEOMAGNETIC POLES FROM LAURENTIA, GONDWANA, BALTICA AND SIBERIA USED FOR RECONSTRUCTION

Pole	Rock unit	Age (Ma)	Plat (°N)	Plong (°E)	A_{95} (°)	1234567 (Q)	References
North China Craton							
O_2	O_2 limestones	-	-31.5	147.7	7.0	1111111 (7)	Huang et al., 1999
O_{1-2}	O_{1-2} limestones	-	-28.8	130.9	12.3	1111110 (6)	Zhao et al., 1992
O_1	O_1 limestones	-	-37.4	144.3	8.5	1111110 (6)	Huang et al., 1999
GC	Kushan and Changshan formations	ca. 500–490*	-31.7	149.6	5.4	1111110 (6)	Huang et al., 1999
ZX	Changhsia Fm	ca. 504–500*	-36.3	147.1	8.1	1111110 (6)	Huang et al., 1999; this study
XZ	**Hsuchuang Fm**	**ca. 505**	**-31.8**	**140.4**	**5.3**	**1111110 (6)**	**This study**
XJ	Xinjin and Wudaotang formations	ca. 514–509*	-18.5	161.9	6.5	1111101 (6)	Huang et al., 1999
Laurentia							
TS	Taum Sauk limestone	ca. 500	3.4	355.1	7.1	1110101 (5)	Dunn and Elmore, 1985
RY	Royer Dolomite	ca. 500	-12.6	337.3	3.5	1111101 (6)	Nick and Elmore, 1990
FM	Florida Mountains auriole	510 ± 5	6.0	349.0	8.0	1110111 (6)	Geissman et al., 1991; Amato and Mack, 2012
TP†	Tapeats Sandstone	ca. 508	-1.7	342.6	2.5	1100111 (5)	Elston and Bressler, 1977
Gondwana							
G510§	Middle/Late Cambrian	ca. 510	-9.6	175.6	4.6	-	McElhinny et al., 2003
Baltica							
NV†	Narva Cambrian sandstone, Russia	ca. 500	34.2	79.8	5.5	0110111 (5)	Khramov and Iosifidi, 2009
Siberia							
KB	Khorbusuonka limestone	ca. 502	41.6	321.8	2.0	1111111 (7)	Gallet et al., 2019

Notes: Plat/Plong–pole latitude/longitude; A_{95}–confidence circle of the pole; Q–quality value (maximum of 7; Van der Voo, 1990); Fm–Formation; Gp–Group; O_1–Lower Ordovician; O_2–Middle Ordovician.

[*]Ages are based on the updated Cambrian bio-stratigraphic and chronostratigraphic framework of the North China Craton (e.g., Zhu et al., 2019).

[†]Pole Latitude/Longitude corrected for inclination shallowing with flattening factor of 0.6 following Torsvik et al. (2012).

[§]Ca. 510 mean pole for Gondwana in NW African coordinates calculated by McElhinny et al. (2003).

8. Table DR3

TABLE DR3. EULER ROTATIONS FOR THE PALEOGEOGRAPHIC RECONSTRUCTION IN THE MIDDLE CAMBRIAN (CA. 505 Ma)

Plate	Latitude (°)	Longitude (°)	Angle (°)
Gondwana (in NW African coordinates) using the pole "G510"	-1.9	83.8	100.2
Laurentia using the pole "TP"	-42.5	5.9	145.8
North China Craton using the pole "XZ"			
Northern hemisphere option	-28.0	-54.1	193.9
Southern hemisphere option	-14.8	58.0	-59.9
Baltica using the pole "NV"	25.9	-71.3	-156.3
Siberia using the pole "KB"	-18	5.1	-148.2

Notes: Poles used for reconstruction are listed in Table DR2. All the rotations are relative to the absolute framework.

9. SUPPLEMENTARY REFERENCES

Amato, J.M., and Mack, G.H., 2012, Detrital zircon geochronology from the Cambrian-Ordovician Bliss Sandstone, New Mexico: Evidence for contrasting Grenville-age and Cambrian sources on opposite sides of the Transcontinental Arch: Geological Society of America Bulletin, v. 124, no. 11-12, p. 1826–1840.

Brock, G.A., Engelbretsen, M.J., Jago, J.B., Kruse, P.D., Laurie, J.R., Shergold, J.H., Shi, G.R., and Sorauf, J.E., 2000, Palaeobiogeographic affinities of Australian Cambrian faunas, in Wright, J.A., et al., eds., Palaeobiogeography of Australian floras and faunas: Association of Australasian Palaeontologists Memoir 23, p. 1–61.

Cawood, P.A., 2005, Terra Australis orogen: Rodinia breakup and development of the Pacific and Iapetus margins of Gondwana during the Neoproterozoic and Paleozoic: Earth-Science Reviews, v. 69, p. 249–279.

Dalziel, I.W.D., 2014, Cambrian transgression and radiation linked to an Iapetus-Pacific oceanic connection?: Geology, v. 42, p. 979–982.

Dunn, W.J. and Elmore, R.D., 1985, Palaeomagnetic and petrographic investigation of tbe Taum Sauk Limestone, southeast Missouri: Journal of Geophysical Research, v. 90, p. 11,469–11,483.

Elston, D.P., and Bressler, S.L., 1977, Paleomagnetic poles and polarity zonation from Cambrian and Devonian strata of Arizona: Earth and Planetary Science Letters, v. 36, p. 423–433.

Fisher, R., 1953, Dispersion on a sphere: Proceedings of the Royal Society of London., v. A217, p. 295–305.

Gallet, Y., Pavlov, V., and Korovnikov, I., 2019, Extreme geomagnetic reversal frequency during the Middle Cambrian as revealed by the magnetostratigraphy of the Khorbusuonka section (northeastern Siberia): Earth and Planetary Science Letters, v. 528, 115823.

Geissman, J.W., Jackson, M., Harlan, S.S., and Van der Voo, R., 1991. Paleomagnetism of Latest Cambrian–Early Ordovician and Latest Cretaceous–Early Tertiary rocks of the Florida Mountains, southwest New Mexico: Journal of Geophysical Research, v. 96, no. B4, p. 6053–6071.

Han, Y.G., Zhao, G.C., Cawood, P.A., Sun, M., Eizenhöfer, P.R., Hou, W.Z., Zhang, X.R., and Liu,

Q., 2016, Tarim and North China cratons linked to northern Gondwana through switching accretionary tectonics and collisional orogenesis: Geology, v. 44, no. 2, p. 95–98.

Huang, B.C., Yang, Z.Y., Otofuji, Y.I., and Zhu, R.X., 1999, Early Paleozoic paleomagnetic poles from the western part of the North China Block and their implications: Tectonophysics, v. 308, no. 3, p. 377–402.

Huang, B.C., Zhou, Y.X., and Zhu, R.X., 2008, Discussion on Phanerozoic evolution and formation of continental China, based on paleomagnetic studies: Earth Science Frontiers, v. 15, no. 3, p. 348–359 [in Chinese with English abstract].

Khramov, A.N., and Iosifidi, A.G., 2009, Paleomagnetism of the Lower Ordovician and Cambrian sedimentary rocks in the section of the Narva River right bank, for the construction of the Baltica kinematic model in the early Paleozoic: Izvestiya Physics Solid Earth, no. 45, p. 465–481.

Li, Z.X., and Powell, C.M., 2001, An outline of the palaeogeographic evolution of the Australasian region since the beginning of the Neoproterozoic: Earth-Science Reviews, v. 53, p. 237–277.

McElhinny, M.W., 1964, Statistical significance of the fold test in paleomagnetism: Geophys. J. R. Astron. Soc., v. 8, p. 338–340.

McElhinny, M.W., Powell, C.M., and Pisarevsky, S.A., 2003, Paleozoic terranes of eastern Australia and the drift history of Gondwana: Tectonophysics, v. 362, no. 1–4, p. 41–65.

McFadden, P.L., 1990, A new fold test for paleomagnetic studies: Geophysical Research Letters, v. 103, p. 163–169.

McFadden, P.L., and McElhinny, M.W., 1990, Classification of the reversal test in palaeomagnetism: Geophysical Journal International, v. 103, no. 3, p. 725–729.

Miao, X., 2015, New paleomagnetic evidence for the development and evolution of the Paleo-Asian Ocean in Late Paleozoic [Master thesis]: China University of Geosciences, Beijing, 51 p. [in Chinese with English abstract].

Nick, K.E., and Elmore, R.D., 1990, Paleomagnetism of the Cambrian Royer dolomite and Pennsylvaniam Collings Ranch conglomerate, southern Oklahoma: an early Paleozoic magnetization and nonpervasive remagnetization by weathering: Geological Society of America Bulletin, v. 102, p. 1517–1525.

Sun, Z., Zeng H., and Zhao, F., 2020a, First occurrence of the Cambrian arthropod Sidneyia Walcott, 1911 outside of Laurentia: Geological Magazine, v. 157, no. 3, p. 405–410.

Sun, Z., Zeng H., and Zhao, F., 2020b, Occurrence of the hurdiid radiodont Cambroraster in the middle Cambrian (Wuliuan) Mantou Formation of North China: Journal of Paleontology, doi: 10.1017/jpa.2020.21.

Sundberg, F.A., Karlstrom, K.E., Geyer, G., Foster, J.R., Hagadorn, J.W., Mohr, T.M., Schmitz, M.D., Dehler, C.M., and Crossey, L.J., 2020, Asynchronous trilobite extinctions at the early to middle Cambrian transition: Geology, v. 48, no. 5, p. 441–445.

Torsvik, T.H., et al., 2012, Phanerozoic Polar Wander, palaeogeography and dynamics: Earth-Science Reviews, v. 114, p. 325–368.

Torsvik, T.H., and Cocks, L.R.M., 2017, Cambrian, in Torsvik, T.H., and Cocks, L.R.M., eds., Earth History and Palaeogeography: Cambridge, UK, Cambridge University Press, p. 85–100.

Van der Voo, R., 1990, The reliability of paleomagnetic data: Tectonophysics, v. 184, p. 1–9.

Xian, H., Zhang, S., Li, H., Xiao, Q., Chang, L., Yang, T., and Wu, H., 2019, How did South China connect to and separate from Gondwana? New paleomagnetic constraints from the Middle Devonian red beds in South China: Geophysical Research Letters, v. 46, no. 13, p. 7371–7378.

Zhao, X., Coe, R.S., Liu, C., and Zhou, Y., 1992, New Cambrian and Ordovician paleomagnetic poles for the north China Block and their paleogeographic implications: Journal of Geophysical Research, v. 97, p. 1767–1788.

Zhu, M., Yang, A., Yuan, J., Li, G., Zhang, J., Zhao, F., Ahn, S.Y., and Miao, L., 2019, Cambrian integrative stratigraphy and timescale of China: Science China Earth Sciences, v. 62, p. 25–60.